Band lineup in amorphous/crystalline silicon heterojunctions and the impact of hydrogen microstructure and topological disorder

T. F. Schulze,* L. Korte, F. Ruske, and B. Rech

Helmholtz-Zentrum Berlin für Materialien und Energie, Institute Silicon Photovoltaics, Kekuléstraße 5, D-12489 Berlin, Germany

(Received 22 December 2010; published 21 April 2011)

We determine the band offsets in amorphous/crystalline silicon [a-Si:H/c-Si{111}] heterojunctions using combined data from photoelectron spectroscopy and surface photovoltage measurements on structures comprising a-Si:H layers with device-relevant thickness (10 nm). Altering the a-Si:H hydrogen (H) content C_H by the choice of deposition conditions, we observe a systematic retreat of the a-Si:H valence band edge leading to an increase of the band gap and the valence band offset ΔE_V with C_H by about 13 meV/at. % H. The discrepancy with the 30–40 meV/at. % H predicted by theory can be consistently explained by the compensating effect of enhanced topological disorder imposed by the increasing density of microvoids as revealed by an analysis of the H microstructure. Thus we highlight the necessity of explicitly including the details of the H configuration in a theoretical treatment of the a-Si:H/c-Si heterojunction.

DOI: 10.1103/PhysRevB.83.165314 PACS number(s): 81.05.Gc, 79.60.Jv, 73.20.At, 71.23.Cq

I. INTRODUCTION

The band offsets in a semiconductor heterojunction (HJ) are a fundamental quantity, determining the distribution of band bending in the structure and affecting the electronic transport across the junction. They appear due to the difference in band gap between the two materials forming the heterostructure. Fundamentally, the exact alignment is defined by the energetic positions of the branch points of the semiconductors' virtual gap states (the so-called charge-neutrality levels).[1–3] If present, interface dipoles or defect states eventually alter the band-structure-derived lineup.

Tuning the band gap of one of the materials offers a unique way to control the behavior of a heterojunction device (i.e., the optical or electrical transport properties) but naturally leads to changes in the band offsets. Depending on the nature of states that are removed or created when altering the band gap, a change in either one or both of the band offsets can occur. Thus, the exact reaction of the band lineup upon tuning the band gap is not trivially anticipated; on the other hand it can heavily affect the electronic behavior of a heterojunction device.[4] Despite the importance of HJ-derived devices such as lasers, transistors, photodetectors, and solar cells, there are only limited data on the connection between tunable material parameters of particularly amorphous materials and the resulting HJ band lineups, and the underlying principles are not thoroughly understood.

In the present study we analyze the amorphous/crystalline silicon [a-Si:H/c-Si{111}] heterojunction, which is formed by growing hydrogenated amorphous silicon onto a crystalline silicon substrate. Due to the structural freedom provided by the adaptability of the amorphous network, a-Si:H allows one to tune the band gap by altering its hydrogen (H) content without severely deteriorating its electronic properties. This structure has tremendous practical importance as it is found in bipolar transistors[5] and high-efficiency solar cells.[6] In microcrystalline silicon, the a-Si:H/c-Si interface is present on a microscopic scale as the boundary between microsized silicon crystallites and the surrounding amorphous matrix, thus affecting the electronic transport in pertinent devices, such as thin-film solar cells.[7]

Controlling the hydrogen content of nominally undoped amorphous silicon [(i)a-Si:H] layers by the choice of conditions during plasma-enhanced chemical vapor deposition, we can vary the (i)a-Si:H band gap within a range of 150 meV, as confirmed by the analysis of spectral ellipsometry data. Observing the schematic band lineup in Fig. 1, it is obvious that the quantities needed to determine the band offsets in the a-Si:H/c-Si structure are the distance of the c-Si and a-Si:H valence band edges from the Fermi energy ($E_{V,\text{c-Si}}$ and $E^{\mu}_{V,\text{a-Si:H}}$), the c-Si equilibrium band bending $e\varphi$, and the a-Si:H band gap. Care has to be taken in distinguishing the a-Si:H optical band gap $E^{\text{opt}}_{g,\text{a-Si:H}}$ (as measured with optical methods) from the mobility band gap $E^{\mu}_{g,\text{a-Si:H}}$ (as determined with electrical techniques), as well as the respective band edges (cf. Fig. 1). Here we define the band offsets as the energetic distances between c-Si band edges and a-Si:H *mobility* edges, as this procedure yields the quantities relevant for electronic transport. The c-Si band edge $E_{V,\text{c-Si}}$ can be readily determined from the conductivity of the crystalline substrate; thus only the a-Si:H valence mobility edge $E^{\mu}_{V,\text{a-Si:H}}$ and $e\varphi$ remain to be measured in order to obtain ΔE_V. With the additional knowledge of the a-Si:H mobility band gap $E^{\mu}_{g,\text{a-Si:H}}$, we can calculate ΔE_C.

Here we probe the valence band (VB) edge in the amorphous bulk with photoelectron spectroscopy (PES), while the c-Si equilibrium band bending is measured using the surface photovoltage (SPV) technique. Thus we are able to monitor the changes in a-Si:H/c-Si band offsets upon tuning the a-Si:H band gap in a device-relevant structure. We find that with increasing $E^{\mu/\text{opt}}_{g,\text{a-Si:H}}$, the valence band offset is enhanced significantly while the conduction band offset stays essentially constant, consistent with the removal of states at the top of the valence band. We rationalize our results in the light of recent theoretical works, and highlight the importance of both hydrogen content *and* hydrogen microstructure, which are found to codetermine the a-Si:H/c-Si band offsets through the effects of increased Si-H bond density and enhanced topological disorder.

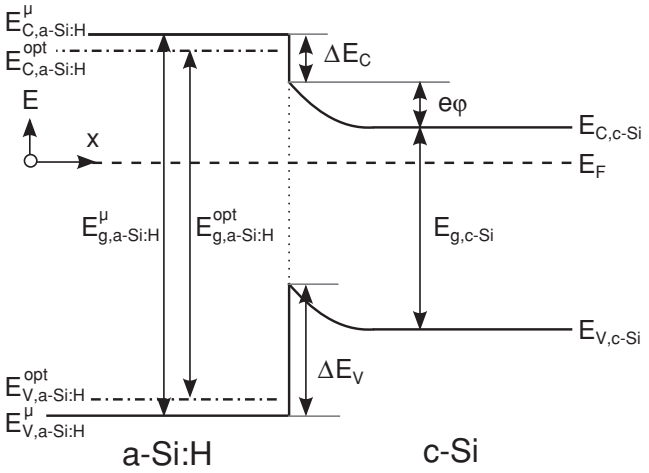

FIG. 1. Schematic of the band lineup in an (i)a-Si:H/(n)c-Si heterojunction in equilibrium. Note that the a-Si:H part of the junction supports only a negligible part of the band bending as the comparably high density of rechargeable states is shielding the electric field built up by the immobile dopant ions in the c-Si. Thus, the valence band offset can be calculated with $\Delta E_V = -E^{\mu}_{V,\text{a-Si:H}} + E_{V,\text{c-Si}} + e\varphi$. Note that in a-Si:H, the optical band gap $E^{\text{opt}}_{g,\text{a-Si:H}}$ (measured with optical methods) has to be distinguished from the mobility band gap $E^{\mu}_{g,\text{a-Si:H}}$ (determined with electrical techniques), as discussed in the text.

II. EXPERIMENTAL DETAILS

A. Amorphous silicon preparation and characterization

The (i)a-Si:H layers were deposited in a conventional 13.56 MHz parallel-plate plasma-enhanced chemical vapor deposition (PECVD) system with a base pressure of 2×10^{-7} mbar, using silane and hydrogen as precursor gases. We compare three different deposition regimes, whose details (pressure p, H dilution ratio $R_H = [H_2]/[SiH_4]$ with the precursor gas flows $[H_2]$ and $[SiH_4]$, electrode distance d_{el}, and power density P) are summarized in Table I. The a-Si:H films were deposited at three different substrate temperatures ($T_{\text{depo}} = 210°\text{C}$, 170°C, or 130°C) on {111}-oriented mirror-polished (n)c-Si with 3 Ω cm resistivity. More details on the preparation methods can be found in Ref. 8. We verified that the structural and electronic properties of the a-Si:H were of state-of-the-art quality, i.e., a valence band tail slope (Urbach energy, E_{0V}) of <70 meV and a dangling bond defect concentration of $<10^{18}\,\text{cm}^{-3}\,\text{eV}^{-1}$. Unlike in previous experimental studies on the a-Si:H/c-Si band offsets, all experimental data were taken on samples with 10 nm a-Si:H thickness, i.e., the thickness typically used in heterojunction transistors and solar cells.

To quantify the H bonding configuration in the a-Si:H layers we measured Fourier-transform infrared absorption spectroscopy (FTIRS) in Brewster-angle transmission mode on a Bruker IFS 66v/S system using symmetrical (i)a-Si:H/(n)c-Si(111)/(i)a-Si:H structures. The H content of the thin layers was determined from the integrated peak intensity of the Si-H stretching modes following the procedure of Langford *et al.*[11] The stretching-mode region was chosen as for the given combination of beam splitter and detector in the FTIRS setup, this wavenumber region has a high signal-to-noise ratio and thus yields the most trusted results.

TABLE I. PECVD deposition parameters of the (i)a-Si:H layers analyzed in the course of this study. For each parameter set, three deposition temperatures were used ($T_{\text{depo}} =$ 210 °C, 170 °C, or 130 °C), yielding a total of 9 different samples.

Name[a]	p (mbar)	R_H	d_{el} (mm)	P (mW/cm^2)
LP	0.5	0	30	9.4
MP	1	10	30	9.4
HP	4	10	20	15.1

[a]cf. Refs. 9 and 10.

In the following we make use of the a-Si:H bulk hydrogen content (C_H), which we define as the vibrational response in the bulk-related IR modes, i.e., discarding the hydrogen bound to the free a-Si:H surface. Further details on the analysis of the H microstructure will be discussed below, and can be found in Refs. 9,10.

Near-ultraviolet PES (NUVPES) in the constant-final-state-yield mode (CFSYS,[12,13]) was applied to determine the a-Si:H valence band edge relative to the Fermi energy and to characterize the a-Si:H valence band tail. Compared to the total-yield PES classically used to study amorphous semiconductors, the CFSYS technique has the advantage that no assumptions concerning the energy dependence of the density of unoccupied states have to be made. The CFSYS spectra are directly proportional to the density of occupied states multiplied by the optical transition matrix element, which is known for a-Si:H.[14] Even though the assumption of an energy-indepedent conduction band density of states (DOS) is reasonable for a-Si:H and in consequence, total-yield PES was successfully applied,[15–17] it is important to remember this fundamental difference.

We measured CFSYS after directly transferring the samples from the high-vacuum PECVD system to the ultrahigh-vacuum analytics chamber to avoid surface contamination. The parameters of the (i)a-Si:H DOS were obtained by fitting a model DOS convoluted with the instrument's transfer function to the PES spectra. Details of this procedure will be discussed below and can also be found in Refs. 8,18.

We measured spectral ellipsometry (SE) on a Woollam VASE system and analyzed the data with model-based fitting. SE was measured in a photon energy range of 1-3.6 eV in order to cover the a-Si:H band edge region. We parametrized the optical response of the a-Si:H layers with a Tauc-Lorentz approach following Jellison *et al.*,[19] as well as with the modified Tauc-Lorentz model of Ferlauto *et al.*[20] While the former comprises a minimum set of fit parameters, the latter includes some specific aspects of amorphous semiconductors such as exponentially decaying band tails. Additionally, the Jellison model is based on the assumption of a constant momentum matrix element for optical transitions, while Ferlauto assumes a constant dipole matrix element. The fits were done with the program RIG-VM (Fraunhofer Institute for Surface Engineering and Thin Films, Germany).[21] We extracted the a-Si:H optical band gap $E^{\text{opt}}_{g,\text{a-Si:H}}$ as a fit parameter from both models, as well as the long-wavelength limit of the dielectric constant for the calculation of the a-Si:H mass density.[22] The errors for the $E^{\text{opt}}_{g,\text{a-Si:H}}$ fit value were determined from the covariance

matrices provided by the Levenberg-Marquardt fitting routine. To verify this estimation, we exemplarily calculated the dielectric functions resulting from the two-fit models for some samples, stochastically varying all fit parameters within their $1\,\sigma$ intervals. We then analyzed Tauc plots[23] of the resulting k functions and verified that the minimum and maximum band gaps estimated from this procedure differed by not more than the fitting error indicated by the fitting routine.

B. The distribution of band bending

To quantify the c-Si band bending in equilibrium we employed the surface photovoltage method.[24] In a dedicated setup (sketched in Fig. 2), a metal-insulator-semiconductor (MIS) structure is formed between a transparent conducting oxide (TCO) on a glass plate serving as front contact, an insulating mica plate, and the a-Si:H/c-Si sample, while a gold-plated chuck provides an Ohmic back contact. The sample is then excited with a short laser pulse (wavelength 904 nm, duration 150 ns, photon flux $10^{19}\,\mathrm{cm}^{-2}\,\mathrm{s}^{-1}$) and the change in surface potential resulting from the redistribution of photogenerated charge carriers is detected via the change in capacitance of the MIS structure. As the photon energy is smaller than the a-Si:H band gap ($E_{\mathrm{phot}} = 1.37\,\mathrm{eV}$), the photogeneration takes place only in the crystalline part of the junction leading to a flattening of the bands and a split-up of the quasi-Fermi levels of electrons and holes ($E_{F,e}$ and $E_{F,p}$ in Fig. 2). The variation in surface potential measured as a photovoltage pulse V_{SPV} corresponds to a change in band bending supported by the c-Si, after correction for the Dember voltage resulting from the difference in mobilities of electrons and holes.[25] Ideally, the illumination intensity is chosen high enough to reach flatband conditions in the sample and the system is in steady state when the laser pulse is switched

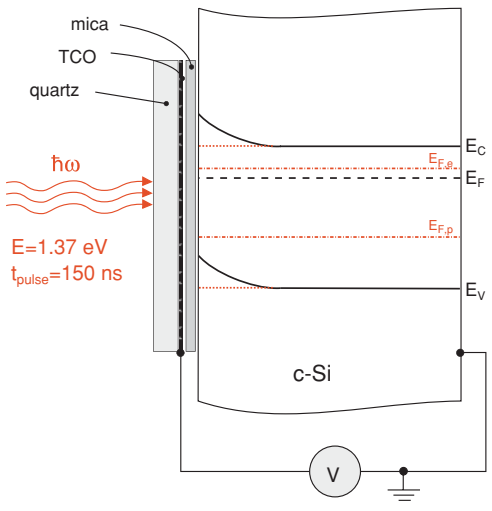

FIG. 2. (Color online) Schematic of the surface photovoltage (SPV) measurement setup. An MIS structure is formed between a transparent conducting oxide (TCO) on a glass plate serving as front contact, an insulating mica plate, and the a-Si:H/c-Si sample. The crystalline silicon is driven into flatband conditions by a short and intense laser pulse, while the change in surface potential is detected capacitively. After correcting the SPV signal for the Dember voltage, it equals the c-Si equilibrium band bending $e\varphi$.

off. Then, the maximum value of the Dember-corrected SPV signal right after the laser pulse, $V_{\mathrm{SPV,corr}}(t = 0)$, directly yields the c-Si band bending in the dark, $e\varphi$. This is the case under high injection conditions, when charge carrier densities $n_{\mathrm{illum}}\, p_{\mathrm{illum}} \gg n_{\mathrm{dark}}\, p_{\mathrm{dark}}$. In our setup, the initial excess charge carrier density is $> 2 \times 10^{17}\,\mathrm{cm}^{-3} \gg N_{\mathrm{doping}}$; thus high injection conditions are fulfilled and we assume $e\,V_{\mathrm{SPV,corr}}(t = 0) = e\varphi$. As generation of electron-hole pairs takes place only in the c-Si, recharging of the a-Si:H defect states should mainly occur through injection of electrons and holes into the thin a-Si:H film, which is supposed to have a negligible effect on $V_{\mathrm{SPV,corr}}(t = 0)$, as these processes are comparably slow and thus only affect the form of the SPV decay transient.[26]

C. Methods for the determination of band offsets

From an experimental point of view, the band offsets in a heterojunction are not trivially accessed. For the a-Si:H/c-Si system under study in this work, two different approaches have been pursued so far.

First, electrical techniques such as capacitance or conductance measurements[27–30] or internal photoemission (IPE)[31,32] were used. The electrical methods to determine HJ band offsets are relatively indirect and often rely on either auxiliary data (affected by uncertainties) or numerical simulations in order to interpret the results. IPE is in principle a direct method and was successfully applied to crystalline heterojunctions (e.g., in III–V systems) or semiconductor-isolator junctions before.[33] For HJs comprising a-Si:H, however, the significant contribution of the gap states to the photoyield leads to difficulties in the interpretation of the data. Consequently, the values obtained by the different authors for ΔE_V with the methods mentioned above differ by a large amount, namely between $\Delta E_V \approx 0$ and $\Delta E_V \approx 0.7\,\mathrm{eV}$ (cf. the compilation of data in Ref. 34). Additionally, most of the studies suffer from incomplete characterization of the a-Si:H layers in terms of composition and structure, which—in the light of the variations imposed by H content, network strain, etc.—results in an additional degree of uncertainty.

A second approach employs photoelectron spectroscopy on ultrathin a-Si:H layers which allows the detection of the signal of the underlying c-Si substrate along with the a-Si:H photoelectrons.[12,18,35] By either extrapolating the band edges of c-Si substrate and a-Si:H film visible in the spectrum to zero or, more sophisticated, fitting a combined a-Si:H and c-Si valence band edge DOS displaced by the band offset energy sought for, this method directly yields the valence band offset. However, it requires a-Si:H layers with thicknesses of only 0.5–3 nm. Unfortunately, the growth of such thin layers is not representative in terms of hydrogen content and amorphous silicon network equilibration,[36] and the remaining density of a-Si:H/c-Si interface defects under ultrathin a-Si:H is large. Thus, the significance of the obtained results for heterojunction devices usually comprising a-Si:H thicknesses of the order of 10 nm is not guaranteed. Consistently, in a recent work based on the PES method, a variation of the a-Si:H/c-Si valence band offset with the thickness of the a-Si:H overlayer was observed for the thickness range accessible with this method.[18] Thus, in the light of the shortcomings of the previously applied

methods, it is important to revisit the a-Si:H/c-Si band offsets in a system with device-relevant a-Si:H thickness.

Additionally, to our knowledge, none of the two mentioned techniques has been used to study the variation in band offsets upon systematically changing the a-Si:H hydrogen content in order to tune its band gap. To fill this gap we present a systematic study on state-of-the-art a-Si:H layers with 10 nm thickness and C_H varying between 12% and 24%. We employ a straightforward method for the determination of HJ band offsets on device-relevant structures, combining photoelectron spectroscopy and surface photovoltage measurements performed on the same samples.

III. EXPERIMENTAL RESULTS

A. The a-Si:H band gap

It is known that the a-Si:H band gap changes upon varying the bulk hydrogen concentration C_H. This effect has been observed experimentally in several studies on thick samples measuring the optical band gap with absorption spectroscopy.[37–39] In a first step we aim at reproducing this trend for (i)a-Si:H layers of 10 nm thickness. To this end we extract C_H from IR absorption spectroscopy and take SE data on the same samples to quantify $E^{opt}_{g,a\text{-Si:H}}$ with the two models mentioned above. Combining these data in Fig. 3, it is obvious that the band gap widening is also present in thin (i)a-Si:H.

Note that while fitting the Ferlauto model to the SE data yields a slightly larger scatter in the $E^{opt}_{g,a\text{-Si:H}}$ fit value and systematically smaller band gaps, the two parametrizations agree well in terms of the overall trend: The a-Si:H band gap widens by approximately 150 meV when the bulk hydrogen content increases from 12% to 24%. Linear fits yield a slope of 11.1 ± 1.2 meV per at. % H for the Jellison model data (dashed red line in Fig. 3), and 12.6 ± 1.5 meV per at. % H for the Ferlauto model (blue dotted line).

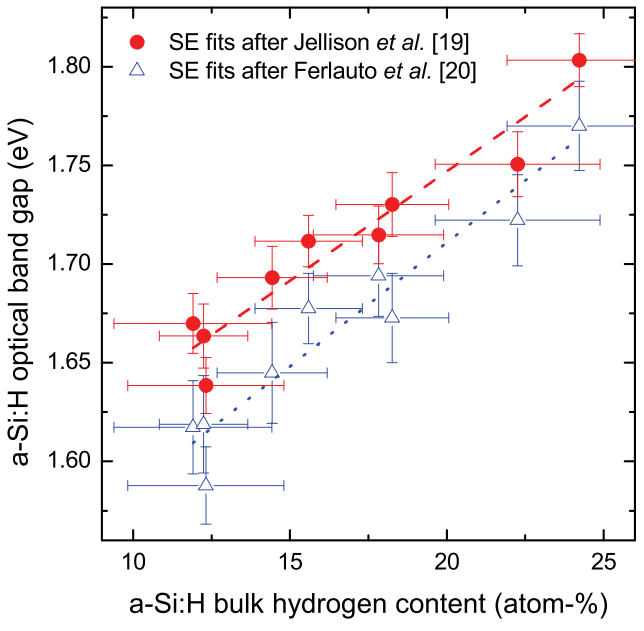

FIG. 3. (Color online) Optical band gap of (i)a-Si:H layers as derived from modeling of SE data and linear fits (lines). Red circles: Tauc-Lorentz model of Jellison *et al.*[19] Blue triangles: Modified Tauc-Lorentz model of Ferlauto *et al.*[20] The latter model leads to a less defined fit value for the band gap due to a higher number of fit parameters and the resulting interdependencies. The offset stems from the different definitions of $E^{opt}_{g,a\text{-Si:H}}$ in the framework of the two models. The slopes of band gap versus H content are compatible.

The differences in fitting results between the two models can be readily explained: The larger errors when employing the Ferlauto parametrization follow from a higher number of fit parameters and the thus resulting cross correlations. The vertical offset of ≈40 meV stems from the different definitions of $E^{opt}_{g,a\text{-Si:H}}$ in the framework of the two models. Ferlauto *et al.* themselves noticed systematically smaller gap values obtained with their model as compared to the optical gaps from Tauc plots[23] of optical absorption spectroscopy data.[20] In the band gap range of our samples, this deviation amounted to about 55 meV, which is reasonably close to the difference between the two models observed here. Thus we can consider the Jellison model to yield band gap estimates compatible with those obtained from optical absorption spectroscopy. As the details of the band tail absorption (which is explicitly included only in the Ferlauto model) are not relevant for our purpose and the band gap fit values obtained with the Jellison model are more robust and compatible with the Tauc gap (thus facilitating comparability to measurements on thick layers), we will rely on the output of the latter model for the remainder of this paper. We further note that the most important SE fit result in the context of our discussion is the *slope* of $E^{opt}_{g,a\text{-Si:H}}$ versus C_H, which we found to be independent of the choice of a-Si:H optical parametrization.

B. The a-Si:H valence band edge

It was found in photoelectron spectroscopy data that the a-Si:H valence band edge moves down in energy upon increasing the hydrogen content.[15] To corroborate these early data on sputtered a-Si:H with measurements on state-of-the-art PECVD films we measured CFSYS on undoped a-Si:H deposited under the same conditions as the FTIRS/SE samples, i.e., with the H content varying from 12% to 24%.

The band edges in amorphous semiconductors are not as well defined as in their crystalline counterparts. The extended states of the valence and conduction band gradually merge into the localized states of the exponentially decaying band tails, rendering the band edges generically blurred. Thus, the energetic positions of the band edges have to be *defined* by choosing an extraction method for a given measurement technique. Consequentially, different competing methods (with more or less rigorous physical foundations) have been used particularly to extract the band gap from optical data, which include extrapolations of the band region (e.g., the Tauc plot[23]) or artificially defined edges as the E_{04} gap. The validity of each of these approaches has been discussed extensively (see, e.g., Refs. 14,40 and references therein).

Here we are interested in the energetic distance of the a-Si:H valence band edge from the Fermi level which is the reference energy in a photoelectron experiment. Principally, different definitions can be chosen in this case as well, such as the extrapolation of the valence band signal to zero or the choice of a distinguished point in the spectrum.

In the following we compare two different techniques: first, the extrapolation of the valence band PES signal toward the abscissa using a square-root function, yielding $E^{\text{ext}}_{V,\text{a-Si:H}}$. This method is motivated by the common approximation of parabolic bands which leads to a square-root law for the DOS and corresponds to a fit of the valence band density of extended states while omitting the contribution of the exponentially decaying localized band tail states to the band edge. Second, the choice of a point 40 meV lower in energy than the transition energy between the exponentially decaying band tail and the valence band, $E^{d}_{V,\text{a-Si:H}}$, as found by fitting a model DOS convoluted with the instrument transfer function to the data.[8,41] This energy corresponds to the valence band mobility edge $E^{\mu}_{V,\text{a-Si:H}}$, i.e., the demarcation energy from extended to localized states in terms of electronic transport, and its definition relative to $E^{d}_{V,\text{a-Si:H}}$ was based on the comparison of internal photoemission data[42] with our own photoconductance data,[41] consistent with other experimental works.[43] When further analyzing the spectra, the mobility edge $E^{\mu}_{V,\text{a-Si:H}}$ would also be used to normalize the model DOS, based on measurements by Street,[44] who found a density of $2 \times 10^{21}\,\text{cm}^{-3}\,\text{eV}^{-1}$ states at $E^{\mu}_{V,\text{a-Si:H}}$. Note, however, that for the band edge definitions used here, no normalization of the model DOS is necessary. Most importantly, the CFSYS spectra are directly *proportional* to the VB DOS,[12,41] which lays a physical foundation for the square-root fit of the spectrum. Thus we can avoid the uncertainties associated with normalization,[17] which leads to a smaller systematic error for our obtained band edge values.

The electrical methods used to determine ΔE_V involve carriers at the mobility edges; thus it is useful to relate our data to the mobility edge for comparability with other approaches. On the other hand, we have to be aware that the band gap defined by the mobility edges ("mobility gap") was found to be systematically wider than the optical band gap (measured, e.g., with absorption spectroscopy) by approximately 160 meV, which has to be taken into account when comparing optical and mobility data.[42]

Observing Fig. 4 we note that the two definitions of the valence band edge lead to values which systematically differ by approximately 90 meV. However, there is the same clear trend for the distance of the valence band edge from the Fermi level increasing by about 150 meV with the hydrogen content. The measured slopes are 11.1 ± 2.8 eV per at. % of H for the mobility edge (red dashed line) and 12.2 ± 2.6 eV per at. % of H for the extrapolated VB edge (blue dotted line); i.e., they are identical within experimental errors.

Interestingly, there is some scatter in the data which is not stemming from the method of VB edge determination, as it has the same form for both data sets. There are some possible reasons for this observation which shall be briefly discussed. First, a possible charging of the sample during the PES measurement generally leads to a displacement of the valence band edge by shifting the reference energy. Although utmost care was taken to avoid such effect, an additional scatter may be introduced by a residual charge accumulating on the sample during measurement. Second, an eventual parasitic surface potential stemming from adsorbates collected during vacuum transfer could also vary from sample to sample as the base pressure in both the PECVD and PES tools is not entirely constant due to the particular chamber history or simultaneously running processes.

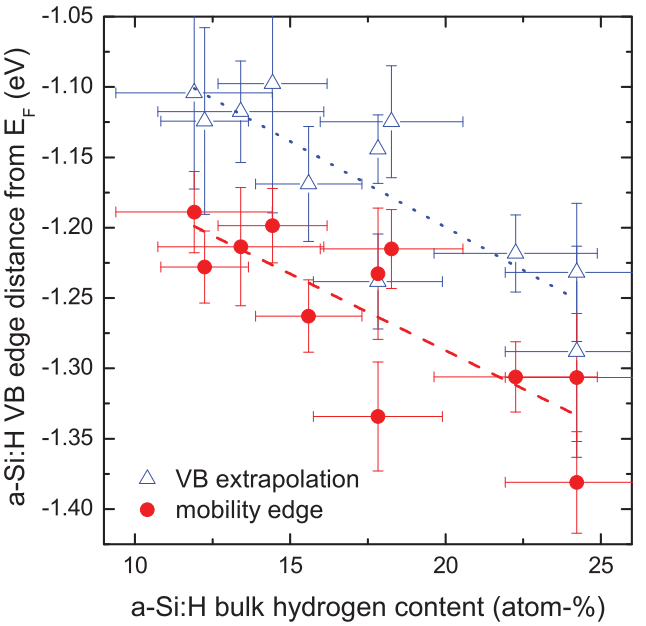

FIG. 4. (Color online) Energetic distance of a-Si:H valence band edges from E_F as determined from the analysis of CFSYS spectra. Blue triangles: Extrapolation of a square-root fit to the a-Si:H valence band PES signal to zero. Red circles: Mobility edge defined after fitting an unnormalized a-Si:H model DOS folded with the instrument's transfer function to the PES data. Both methods yield similar slopes as obtained from linear fits (lines).

Notwithstanding the scatter in the data, the increase in $E^{\mu/\text{ext}}_{V,\text{a-Si:H}}$ with the hydrogen content is pronounced, identical for both band edge definitions and consistent with the data on sputtered a-Si:H.[15] The discrepancy of ≈90 meV between the mobility edge and the band extrapolation-derived edge can be readily explained from the different band edge definitions. Interestingly, the increase in $E^{\mu/\text{ext}}_{V,\text{a-Si:H}}$ is of the same magnitude as the widening of the band gap within experimental errors (cf. Fig. 3). If the gap widening was entirely due to a retreat of the valence band relative to E_F, this would lead to the expectation that predominantly the valence band offset is changing upon varying the H content as can be seen from Fig. 1. This speculation shall be verified in the following, making use of surface photovoltage measurements which probe the band bending in the c-Si toward the heterointerface, the quantity missing to calculate the band offsets from the band edge positions.

C. The a-Si:H/c-Si band offsets

It is obvious from Fig. 1 that based on a known distance of the c-Si VB edge from E_F (defined by the doping concentration) and a measured valence band edge in the a-Si:H bulk, the band offsets can be precisely obtained by the equation

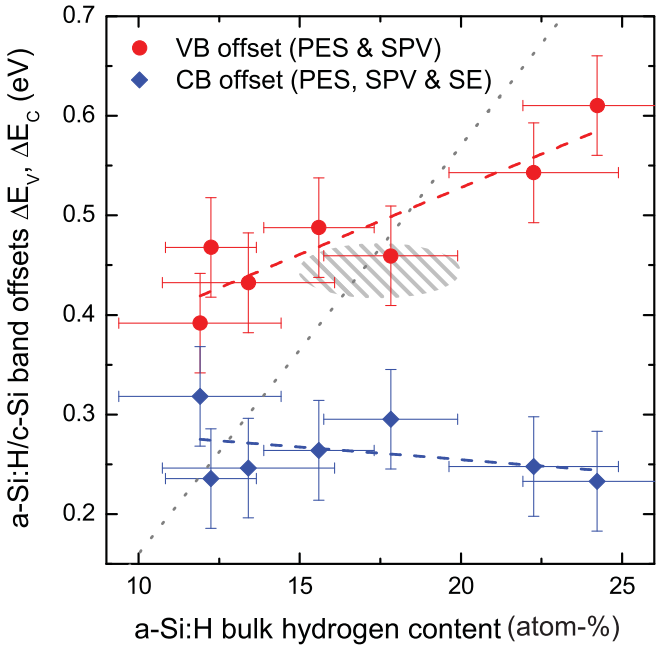

FIG. 5. (Color online) Valence band offsets of (i)a-Si:H/(n)c-Si heterostructures as derived from the combination of PES and SPV data measured on the same samples (red circles). When taking into account the band gap as obtained from the SE fits, the conduction band offset can be calculated as well (blue diamonds). Note that the offsets were obtained based on the a-Si:H mobility edges. Dashed lines are linear fits, the gray hatched area marks the data point of Sebastiani *et al.*,[12] while the gray dotted line is the prediction for the valence band offset by van de Walle *et al.*[45]

$\Delta E_V = -E^{\mu}_{V,\text{a-Si:H}} + E_{V,\text{c-Si}} + e\varphi$ when the amount and distribution of equilibrium band bending $e\varphi$ in the structure is known. Due to the large density of rechargeable states in a-Si:H found in the band tails and the dangling bond defects in the band gap (gap DOS of the order of $10^{17}\,\text{cm}^{-3}\,\text{eV}^{-1}$), the electric field stemming from the immobile dopant ions in the c-Si is shielded in the a-Si:H already close to the heterointerface. The a-Si:H part of the junction will therefore only support a negligible fraction of the overall band bending.[46] Thus, the Dember-corrected SPV signal, identical to the equilibrium band bending in the c-Si, $e\varphi$, is assumed to be equal to the *total* band bending in the structure (as sketched in Fig. 1). We measured SPV on the PES samples to obtain $e\varphi$ in the samples with known VB edge in the a-Si:H bulk. Doing so, we end up with a consistent set of data to calculate the valence band offset, which we analyze in terms of its variation with the H content.

Figure 5 shows the obtained offset of the a-Si:H VB mobility edge from the c-Si VB (ΔE_V) versus the (i)a-Si:H bulk hydrogen content C_H, again assuming that the H content measured on the FTIRS/SE samples is representative for the nominally identical PES samples. The valence band offset increases pronouncedly with C_H, the linear fit of the data (red dashed line) yielding a slope of 13.4 ± 2.8 eV per at. % H. We then combine the PES and SPV data with the optical band gap obtained from SE, adding 160 meV to account for the difference between mobility and optical gap,[42] to calculate the offset between a-Si:H conduction band (CB) mobility edge and c-Si CB (blue data points and dashed line representing a linear fit). The slope of the fit is -2.5 ± 2.7 meV per at. % H, i.e., compatible with zero.

Thus the data support a variation in predominantly the valence band offset upon widening of the a-Si:H band gap by increased hydrogen incorporation. For comparison, the value for the VB offset obtained by Sebastiani *et al.*[12] on PECVD-deposited a-Si:H with 15% to 20% H content is shown (gray hatched area), agreeing reasonably well with our samples of similar H content. The gray dotted line is a calculation of ΔE_V versus C_H by van de Walle *et al.*,[45] which will be discussed below.

IV. DISCUSSION

A. Comparison to experimental works

The variation of the a-Si:H optical band gap with C_H measured on our 10 nm samples is consistent with previous results on thick layers. Cody *et al.*[38] found a slope of 14.8 meV per at. % of hydrogen, while Kaniadakis reports 12.7 meV per at. %,[39] which is compatible with our value within experimental errors. Freeman *et al.*[37] found a slightly higher slope (≈20 meV per at. % H); however their samples were sputtered and due to the large range of deposition conditions covered in their study displayed even differing values for the band gap for identical H content. In consequence, the error bar on this value is certainly large.

Additional support for our data comes from the extrapolation to zero H content, which is suggested by the linearity of the data. We extract a value of 1.52 ± 0.02 eV for pure a-Si, which is reasonably close to the reported ≈1.4 eV for annealed a-Si samples.[47]

Early UV photoelectron spectroscopy experiments showed a retreat of the valence band edge by ≈0.8 eV for sputtered a-Si:H with a H content of 50% as compared to sputtered a-Si, while the position of the Fermi level relative to the core level peaks remained essentially constant, thus consistent with a removal of states at the top of the valence band.[15] PES measurements by the same group on a-Si:H layers prepared by PECVD showed a similar recession as compared to a-Si; the H content of these a-Si:H layers was however not exactly stated.[16] A rule-of-thumb calculation based on the sputtered a-Si:H data[15] assuming a linear retreat of the VB with the H content (although no intermediate H concentrations were explicitly analyzed in the pertinent study) would yield a slope of 11–12 meV per at. % H, which is surprisingly close to our measured value of 11.1 ± 2.8 meV (cf. Fig. 4).

To our knowledge, there is only one experimental study where the band offsets of silicon-based heterojunctions were systematically varied. It was carried out on hydrogenated amorphous silicon carbide/crystalline silicon heterojunctions with NUVPES on ultrathin layers.[35] The authors observed an increase of the a-$Si_{1-x}C_x$:H/c-Si valence band offset from 0.44 ± 0.02 eV found for pure a-Si:H with 15%–20% hydrogen content to 0.95 eV for a-$Si_{0.5}C_{0.5}$:H/c-Si. The H content of the alloyed samples was not specifically analyzed in this study, although a competing incorporation of H and C during growth was previously observed which, in turn, affects the band gap widening.[48,49] Further, there

are no theoretical studies on which an analysis of the a-$Si_{1-x}C_x$:H/c-Si heterojunction could be based. The most simple system to study the effect of compositional variation on the band gap and offsets is surely the unalloyed a-Si:H/c-Si heterojunction, for which some recent theoretical studies are available for comparison. In the next section we will discuss our data in the light of simulation results on the a-Si:H band edges and a-Si:H/c-Si band offsets.

B. Comparison to theory

Theoretical studies on the band structure of a-Si:H qualitatively agree on the band gap widening being caused by a retreat of the valence band edge upon increased hydrogen content, while the conduction band edge stays essentially constant.[50–52] In a simplified picture, this can be explained by the replacement of weak Si-Si bonds forming the top of the valence band by inclusion of hydrogen to form more stable (thus energetically deeper Si-H bonds). The more subtle aspects of the problem such as the chemical nature of the Si-H bonds and topological statistics render this matter more complicated but are beyond the scope of this discussion.

Across the different studies and their theoretical approaches, the calculated slopes of the VB retreat differ. The reported values range from ≈15 meV per at. % hydrogen (close to our measured value) to 40 meV, with the newer works yielding higher slopes. Additionally, it must be noted that the calculated a-Si:H band gaps are mostly too small, as is often the case for calculated band structures.

For the theoretical treatment of the a-Si:H/c-Si heterojunction, there exist two different approaches: While the older studies comprise separate computational treatment of the two phases forming the heterojunction,[45,53] more recent publications attempt a microscopic simulation of the heterointerface itself with the goal of gaining insight in both structural and electrical properties of the junction.[54,55] Although promising from the conceptional point of view, the latter approach seems, at the time being, to suffer from stability problems (amorphization of the c-Si phase or crystallization of the a-Si:H) and does not fully reproduce the essential electronic features of the a-Si:H/c-Si system (such as a low DOS in the band gap). Therefore the former studies still seem to represent a safer ground for comparison to experimental data.

The work of Allan *et al.*[53] is based on "hydrogenation" of the Wooten-Winer-Weaire model for a-Si.[56] It features essential properties of a-Si:H such as a gap widening as compared to a-Si and exponentially decaying band tails with realistic slopes. The slope of the band gap versus H concentration is steep for the lowest H contents (as also observed experimentally[37]) and converges to a quasilinear increase for $C_H > 3\%$, however with a slope as high as 34 meV per at. %. The authors attributed this discrepancy in the experimentally observed slope to the fact that at the low H contents featured in the model ($C_H < 8\%$), the hydrogenation still mainly affects the localized states in the band tails which would lead to increased widening of the gap as compared to more delocalized states. Based on the similar bond angles for their a-Si:H model as compared to c-Si and the resulting similar hybrid orbital energies, the authors argue in favor of a vanishing dipole contribution at the heterointerface and calculate the valence band offset by simply combining the energetic positions of the band edges, yielding $\Delta E_V = 0.36$ eV at ≈8% hydrogen content. This value is reasonably close to our results extrapolated to lower H content; however it is not stated how the VB offset evolves upon band gap increase.

The most comprehensive theoretical study on the band offsets in a-Si:H/c-Si was conducted by van de Walle and Yang.[45] They combined their own "model solid theory"[57] with an *ab initio* pseudopotential calculation (density-functional theory in local-density approximation) to derive the a-Si:H properties[58] and also assumed the absence of interface-specific dipoles. This approach yields a VB offset of 0.2 eV for 11% H content and a slope of ΔE_V with C_H of 40 meV per at. % hydrogen. This prediction clearly contradicts our data, as is obvious in Fig. 5 when comparing the gray dotted line with our data for the VB offset.

In an attempt to explain the discrepancy between calculations and our data we will first analyze the possible impact of interface dipoles, which was neglected in the theoretical approaches discussed above. In modern theories of semiconductor HJ band alignment, the influences on the band offsets are separated into intrinsic contributions stemming from the complex band structure of the two materials forming the HJ, and extrinsic dipoles resulting from a difference in electronegativity or interface-bound defect states.[1,3] There is agreement that the Si-Si bonds spanning the actual heterointerface are nonpolar; however there is a possible shift in the band offsets due to a dipole contribution from polar Si-H bonds at the interface ($\Delta_{Si\text{-}H}$) and from Si dangling bonds carrying charges (Δ_{db}). A recent estimation of the magnitude of both effects yielded a possible $\Delta_{Si\text{-}H,max} = 90$ meV and $\Delta_{db,max} = 1.1$ eV in the geometrical limits, i.e., for a 100% coverage of the c-Si surface with Si-H bonds or a fully unsaturated c-Si surface (7×10^{14} eV^{-1} cm^{-2} surface defect states).[18] Here we know that the difference in H content across the variety of samples is 15 at. %, which should be the range in which the Si-H bond density at the heterointerface varies; thus the impact of $\Delta_{Si\text{-}H}$ is marginal (<15 meV). With photoconductance decay measurements, the dangling bond density at the a-Si:H/c-Si interface was found to vary between ≈10^{13} eV^{-1} cm^{-2} and ≈10^{11} eV^{-1} cm^{-2} for the layers under study here, depending on the deposition conditions[9,10] (consistent with older results from SPV measurements[59]). Thus, Δ_{db} across the range of samples could amount to only ≈13 meV in our case. Hence we can state that a possible contribution of interface dipoles cannot not significantly affect the behavior of the band offsets in our samples and therefore does not explain the observed difference between calculations and our data.

In the following we will argue in favor of a different explanation: Our data suggest that a competing influence on the band gap of both increased Si-H bond density and enhanced a-Si:H network disorder resulting from the details of H incorporation, not accounted for in the calculations, is responsible for the reduced measured slope of the valence band retreat.

C. Impact of disorder and hydrogen microstructure

1. Topological disorder

In a classic paper on optical absorption in a-Si:H, Cody *et al.* argued that the principal origin for the varying band

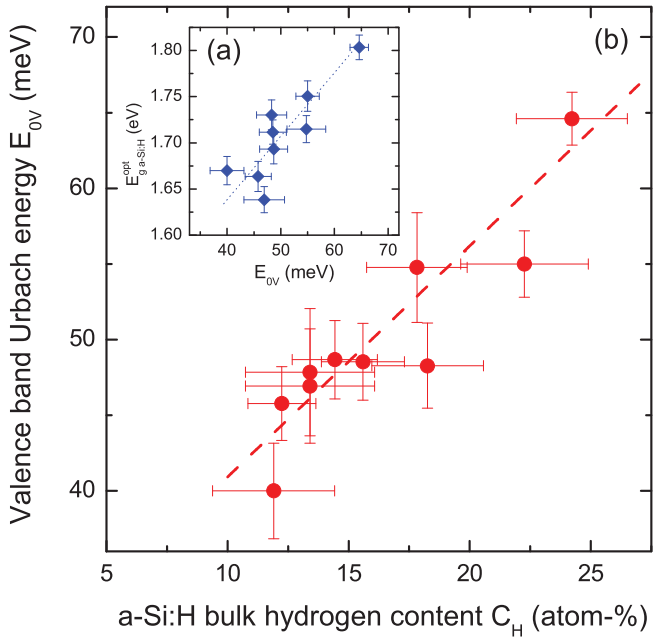

FIG. 6. (Color online) (a) Variation of the a-Si:H optical band gap when plotted against the valence band tail slope (Urbach energy) E_{0V} as derived from photoelectron spectra. The dotted line is a guide to the eye. (b) Increase of the Urbach energy E_{0V} (reflecting topological disorder and strain in the amorphous network) upon increased H incorporation, and linear fit to the data (red dashed line).

gap of a-Si:H was not the hydrogen replacing Si-Si by Si-H bonds but the effect of topological disorder.[60] This argument was based on a universal connection between Urbach energy E_{0V} and band gap $E^{\text{opt}}_{g,\text{a-Si:H}}$ which they observed in a sample series where initially incorporated H was driven out by successive heating. They observed $E^{\text{opt}}_{g,\text{a-Si:H}}$ to collapse from about 1.7 eV to 1.5 eV due to the creation of localized states in the band tail upon H evolution, while E_{0V} increased from about 60 meV to 90 meV. Interestingly, the band tail retained its exponential shape across the whole range of data. The fact that the same $E^{\text{opt}}_{g,\text{a-Si:H}}$ versus E_{0V} trend also held for the temperature dependence $E_g(T_{\text{meas}})$ versus $E_{0V}(T_{\text{meas}})$ for all analyzed samples was taken as evidence that the increased disorder (either of thermal nature from raising the temperature or of compositional nature from driving out the hydrogen) is the unifying origin for the variations in the band gap.

Plotting our optical band gap data from SE versus the Urbach energy E_{0V} as measured with CFSYS in Fig. 6(a), we observe a pronounced *increase* of the gap with the Urbach slope. At first glance this result is contradicting the data shown by Cody and points toward more subtle aspects governing the interplay between E_{0V}, C_{H}, and E_g. However, it must be noted that while Cody was driving out the H of an amorphous network already fixed in the moment of deposition, we control the H content *a priori* by changing the deposition conditions. Thus, the Si network is able to accommodate a lower H content by changing its topology, without creating the same amount of localized states contributing to a broader band tail and smaller gap as was observed by Cody. Our data now suggest on the other hand that H incorporation itself is a source of disorder, as the Urbach energy systematically increases with C_{H} [shown in Fig. 6(b)]. Thus, to reconcile Cody's observation of a band gap reduction with E_{0V} and our opposite result, we must assume at least *two* contributions of separate physical origin to the variation of the band gap: H content *and* topological disorder, which are—as obvious from Fig. 6—however practically connected by the enhanced disorder following from increasing H incorporation (for the H contents under study here). This means that the retreat of the valence band by increased Si-H bond density is partly compensated by the broadened and shifted valence band tail due to increased disorder resulting from the incorporation of hydrogen during PECVD growth.

In the following, we will briefly look into the details of hydrogen incorporation in order to identify the possible *structural* origin of the disorder increasing with the H content.

2. The hydrogen microstructure

It is commonly known that H can be incorporated into a-Si:H in a large variety of topological configurations, covering isolated monohydrides, the termination of dangling Si bonds in mono- and multivacancies and platelets, as well as polysilane chains and H-decorated nano- or even microsized voids. The experimental signatures of these structures in different techniques and their respective significance for structural and electronic properties of a-Si:H have been widely discussed (see, e.g., Refs. 62–66 and references therein). A powerful means in the analysis of H microstructure is IR absorption spectroscopy, where different H configurations can be distinguished by their vibrational spectra.[11,62,66] Concerning the IR signature, there is agreement that the above mentioned topological configurations can be categorized into "compactly incorporated monohydrides" (isolated Si-H and mono- and multivacancies), giving rise to the so-called low-frequency stretching mode around 2000 cm^{-1} (LSM), and "clustered monohydrides" on the inner surfaces of voids, giving rise to a high-frequency stretching mode around 2090 cm^{-1} (HSM).[63,67] The existence of a medium-frequency stretching mode around 2040 cm^{-1} indicating platelet structures[66] and the ambivalence of the 2090 cm^{-1} absorption peak, being often associated with dihydrides as well,[62,67] are under discussion.

Observing Fig. 7(a), where the concentrations of H found in both LSM and HSM are plotted versus the total H content, we note that the increase of the bulk H content is entirely due to the H configuration giving rise to the HSM. In order to corroborate the interpretation of the HSM being indicative of H-decorated voids, we analyzed the mass density of the films, which we calculated using a Clausius-Mossotti approach[22] from the refractive index in the long-wavelength limit. The result in Fig. 7(b) shows a pronounced loss in film density with increased H incorporation. The slope of the decrease is much higher than what would be expected for the compact hydrogen configurations,[66] which underpins the association of the HSM with Si-H decorating voids. Additional support comes from the analysis of the mass deficiency, i.e., the density loss relative to a-Si, defined as $f_m = 1 - \rho/\rho_{\text{a-Si}}$ with $\rho_{\text{a-Si}} = 2.287\,\text{g/cm}^3$. The decoration of the inner surfaces of microscopic voids in a-Si:H resulting in the HSM in the IR spectra must lead to an increase of the HSM signal with the void *volume*, which is

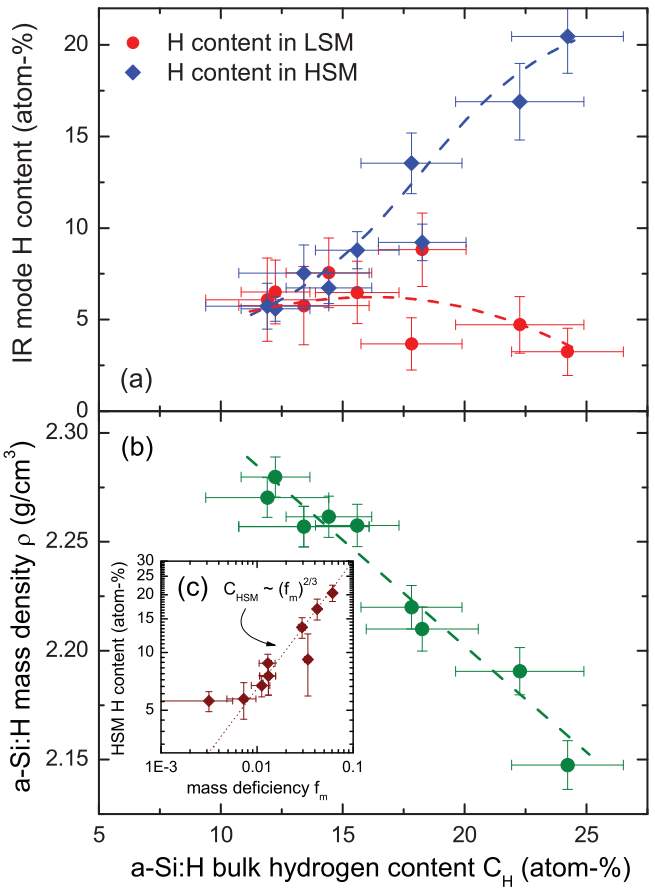

FIG. 7. (Color online) (a) Hydrogen concentration giving rise to the low-frequency stretching mode (LSM) and high-frequency stretching mode (HSM), as explained in the text, versus total bulk H content C_H. It is obvious that the increase of C_H is almost entirely due to the HSM. Dashed lines are guides to the eye. (b) Mass density ρ of a-Si:H films as calculated from FTIRS and SE data versus total bulk H content. The dashed line is a guide to the eye. (c) HSM hydrogen content shown over the mass deficiency f_m as explained in the text and power-law fit (dotted line). The exponent of 2/3 fosters the idea of the HSM being related to Si-H bonds decorating the inner surfaces of microscopic voids (whose volume is proportional to f_m).[61]

proportional to the mass deficiency f_m, to the power of 2/3.[61] Indeed, in Fig. 7(c) it can be seen that $C_{H,HSM}$ scales with f_m according to a power law with an exponent of 2/3.

The general trends in our data are in very good agreement with the data of Smets *et al.*, who analyzed a large number of thick a-Si:H films made by the expanding thermal plasma technique.[61,66] The dominant HSM for a-Si:H films with higher H content was also observed for PECVD films in the μm thickness range by Manfredotti *et al.*[64] This, and the fact that the band gap widening per at. % hydrogen is of the same order as for several other studies, leads us to the conclusion that our samples are typical for the higher H content range (despite their small thickness) and the effects described so far are not due to a somewhat pathological nature of the samples.

Note that it was observed that the a-Si:H density has a considerable impact on the energetic position of the valence band, moving it up in energy with decreasing density.[45] The effect was quantified as $\Delta E = 2.46 f_m$[eV]. In our case this would mean that the predicted slope of the VB retreat ($\approx$40 meV per at. %) would be reduced by approximately $\approx$12 meV per at. % due to the loss in density accompanying the increased C_H. However, we know that the density loss is caused by the increasing presence of voids and therefore does *not* denote a density loss in the bulk of the amorphous network. However, what is relevant for the band offsets is *only* the local bulk density at the interface in void-free regions.[45] Thus, the density effect does *not* account for the discrepancy between calculated and observed band lineup, as we must point out.

Thus we can state two main results at this stage: First, in terms of H content, the samples with $C_H > 12\%$ are characterized by an approximately constant contribution from distributed monohydrides and a strongly increasing phase of clustered-monohydride-decorated voids. Second, the clear trends of the different a-Si:H properties versus the bulk H content (band gap, VB retreat) must therefore be associated with the clustered-H phase, while the reduced density alone does *not* account for the observed slopes. In the last section, we try to link the behavior of the a-Si:H properties to the microscopic structure imposed by an increased contribution of voids.

3. *Interplay of voids, disorder, and electronic structure*

The connection between topological disorder and the band tail states in amorphous silicon was established on a fundamental level: A distribution of bond angles or lengths differing from the c-Si equilibrium value suffices to create exponentially decaying band tails.[51,68] More recently, the valence band tail was identified as being composed of short Si-Si bonds,[69,70] which form filamentary structures in the amorphous network.[71] A recent theoretical work on void-containing a-Si:H revealed the same filamentary structures starting predominantly from the inner surfaces of voids, which were identified as introducing additional strain or disorder in the a-Si:H network.[72] In the light of these results, the observed increase of E_{0V} with the HSM hydrogen content can be consistently explained: Quite counterintuitive at first glance, the appearance of voids does not lead to a relief of strain in the amorphous network (as could be anticipated due to the additional degrees of freedom offered by an empty volume), but creates additional strain, again manifesting in filamentary structures of short bonds that constitute the valence band edge in compact a-Si:H. As a consequence, the less pronounced retreat of the valence band edge upon H incorporation with respect to calculations taking into account *only* the replacement of Si-Si bonds by Si-H (without accompanying increase of strain or disorder due to the topological consequences of increased H incorporation) can be understood through the compensating effect of increased topological disorder associated with filaments of strained bonds attached to the inner surfaces of H-decorated voids.

Having analyzed the interplay of H incorporation, strain/disorder, and the consequences for the a-Si:H band structure and a-Si:H/c-Si band lineup, it is obvious that future theoretical treatments of the a-Si:H/c-Si interface should explicitly include the subtleties of the H microstructure and its variation across the a-Si:H compositional phase diagram.

V. CONCLUSIONS

We have shown that upon increasing the a-Si:H hydrogen content C_H in a-Si:H/c-Si heterojunctions with 10 nm a-Si:H layer thickness, a systematic retreat of the a-Si:H valence band edge leads to a widening of the band gap and an increase of the valence band offset at the heterojunction with a slope of ≈13 meV/at. % H. For a typical range of a-Si:H hydrogen content, previous results for the VB offset obtained by photoelectron spectroscopy on ultrathin layers are confirmed.[12,18] While the general trend of $E^{\mu}_{V,\text{a-Si:H}}$ versus C_H is consistent with previous experimental and theoretical works, we note a discrepancy between particularly the newer calculations and our data in terms of the slope of the VB retreat. Based on the known interface defect and bulk hydrogen densities of the a-Si:H layers we can rule out a dominant contribution from interface dipoles as being responsible for the difference between calculations and measurement. The analysis of the hydrogen microstructure in our a-Si:H layers however suggests that the increasing contribution of voids, which leads to enhanced topological disorder as reflected in a broadened VB tail, counteracts the widening of the gap caused by the increased density of Si-H bonds, thus reducing the slope of the VB retreat. This effect seems to be a generic feature of the higher H content range of a-Si:H samples ($C_H >$ 10 at. %), as we conclude from the compatibility of our measured slope with pertinent data. This highlights the necessity of explicitly modeling the changes in H microstructure and resulting Si network topology when analyzing the a-Si:H/c-Si interface properties. Hopefully, future simulations will be able to incorporate this aspect which may help to reconcile the predicted slope of the valence band retreat with our data.

ACKNOWLEDGMENTS

We thank H. N. Beushausen, C. Leendertz, F. Käß, T. Lussky, and E. Conrad for experimental support and M. Schmidt for valuable discussions. This work has been partially funded by the European Commission through the FP7 project "Heterojunction Solar Cells Based on a-Si:H/c-Si" (HETSI), Grant Agreement No. 211821.

*tim.schulze@helmholtz-berlin.de

[1] J. Tersoff, Phys. Rev. B **30**, 4874 (1984).
[2] C. Tejedor and F. Flores, J. Phys. C **11**, L19 (1978).
[3] W. Mönch, *Semiconductor Surfaces and Interfaces*, Vol. 26 of Springer Series in Surface Sciences (Springer, Berlin, Heidelberg, New York, 1995), 2nd ed.
[4] F. Capasso and G. Margaritondo, editors, *Heterojunction Band Discontinuities—Physics and Device Applications* (North-Holland, Amsterdam, 1987).
[5] M. Ghannam, J. Nijs, R. Mertens, and R. DeKeersmaecker, in *International Electron Devices Meeting* (IEEE, New York, 1984), Vol. 30, pp. 746–748.
[6] M. Tanaka, M. Taguchi, T. Matsuyama, T. Sawada, S. Tsuda, S. Nakano, H. Hanafusa, and Y. Kuwano, Jpn. J. Appl. Phys. **31**, 3518 (1992).
[7] O. Vetterl, F. Finger, R. Carius, P. Hapke, L. Houben, O. Kluth, A. Lambertz, A. Mueck, B. Rech, and H. Wagner, Sol. Energy Mater. Sol. Cells **62**, 97 (2000).
[8] L. Korte and M. Schmidt, J. Non-Cryst. Solids **354**, 2138 (2008).
[9] T. F. Schulze, H. N. Beushausen, C. Leendertz, A. Dobrich, B. Rech, and L. Korte, Appl. Phys. Lett. **96**, 252102 (2010).
[10] T. F. Schulze, H. N. Beushausen, C. Leendertz, A. Dobrich, T. Hannappel, L. Korte, and B. Rech, in *Defects in Inorganic Photovoltaic Materials*, Vol. 1268 of MRS Symposia Proceedings (Materials Research Society, Warrendale, 2010), pp. EE01–07.
[11] A. A. Langford, M. L. Fleet, B. P. Nelson, W. A. Lanford, and N. Maley, Phys. Rev. B **45**, 13367 (1992).
[12] M. Sebastiani, L. Di Gaspare, G. Capellini, C. Bittencourt, and F. Evangelisti, Phys. Rev. Lett. **75**, 3352 (1995).
[13] M. Schmidt, A. Schoepke, L. Korte, O. Milch, and W. Fuhs, J. Non-Cryst. Solids **338–340**, 211 (2004).
[14] W. B. Jackson, S. M. Kelso, C. C. Tsai, J. W. Allen, and S.-J. Oh, Phys. Rev. B **31**, 5187 (1985).
[15] B. von Roedern, L. Ley, and M. Cardona, Phys. Rev. Lett. **39**, 1576 (1977).
[16] B. von Roedern, L. Ley, M. Cardona, and F. W. Smith, Philos. Mag. B **40**, 433 (1979).
[17] K. Winer and L. Ley, Phys. Rev. B **36**, 6072 (1987).
[18] L. Korte and M. Schmidt, J. Appl. Phys. **109**, 063714 (2011).
[19] J. G. E. Jellison and F. A. Modine, Appl. Phys. Lett. **69**, 371 (1996).
[20] A. S. Ferlauto, G. M. Ferreira, J. M. Pearce, C. R. Wronski, R. W. Collins, X. Deng, and G. Ganguly, J. Appl. Phys. **92**, 2424 (2002).
[21] A. Pflug, RIG-VM *Simulation System* (Fraunhofer IST, Braunschweig), [http://www.simkopp.de/rvm/].
[22] Z. Remes, M. Vanecek, P. Torres, U. Kroll, A. H. Mahan, and R. S. Crandall, J. Non-Cryst. Solids **227–230**, 876 (1998).
[23] J. Tauc, R. Grigorovici, and A. Vancu, Phys. Status Solidi **15**, 627 (1966).
[24] K. Heilig, Solid State Electron. **21**, 975 (1978).
[25] H. Dember, Z. Phys. **32**, 554 (1932).
[26] L. Korte, A. Laades, K. Lauer, R. Stangl, D. Schaffarzik, and M. Schmidt, Thin Solid Films **517**, 6396 (2009).
[27] J. M. Essick and J. D. Cohen, Appl. Phys. Lett. **55**, 1232 (1989).
[28] T. Unold, M. Rösch, and G. H. Bauer, J. Non-Cryst. Solids **266–269**, 1033 (2000).
[29] A. Gudovskikh, S. Ibrahim, J.-P. Kleider, J. Damon-Lacoste, P. R. i Cabarrocas, Y. Veschetti, and P.-J. Ribeyron, Thin Solid Films **515**, 7481 (2007).
[30] J. P. Kleider and A. S. Gudovskikh, in *Amorphous and Polycrystalline Thin-Film Silicon Science and Technology*, Vol. 1066 of MRS Symposia Proceedings (Materials Research Society, Warrendale, 2008), pp. A04–01.
[31] M. Cuniot and Y. Marfaing, Philos. Mag. B **57**, 291 (1988).
[32] N. Lequeux and M. Cuniot, J. Non-Cryst. Solids **114**, 555 (1989).
[33] V. V. Afanas'ev, *Internal Photoemission Spectroscopy: Principles and Applications*, 1st ed. (Elsevier, Oxford, 2008).
[34] C. Bittencourt and F. Alvarez, in *Amorphous Silicon and its Alloys*, edited by T. Searle (INSPEC, London, 1998), chap. 3.8, pp. 174–179.

[35]T. M. Brown, C. Bittencourt, M. Sebastiani, and F. Evangelisti, Phys. Rev. B **55**, 9904 (1997).
[36]H. Fujiwara, Y. Toyoshima, M. Kondo, and A. Matsuda, Phys. Rev. B **60**, 13598 (1999).
[37]E. C. Freeman and W. Paul, Phys. Rev. B **20**, 716 (1979).
[38]G. D. Cody, C. R. Wronski, B. Abeles, R. B. Stephens, and B. Brooks, Sol. Cells **2**, 227 (1980).
[39]G. Kaniadakis, *Properties of Amorphous Silicon* (INSPEC, London, 1989).
[40]G. D. Cody, in *Amorphous and Nanocrystalline Silicon Science and Technology*, Vol. 862 of MRS Symposia Proceedings (Materials Research Society, Warrendale, 2005), p. A1.3.1.
[41]L. Korte, Ph.D. thesis, Philipps-Universität Marburg, 2006.
[42]C. R. Wronski, S. Lee, M. Hicks, and S. Kumar, Phys. Rev. Lett. **63**, 1420 (1989).
[43]T. Tiedje, J. M. Cebulka, D. L. Morel, and B. Abeles, Phys. Rev. Lett. **46**, 1425 (1981).
[44]R. A. Street, Phys. Rev. B **43**, 2454 (1991).
[45]C. V. de Walle and L. H. Yang, J. Vac. Sci. Technol. B **13**, 1635 (1995).
[46]F. Rubinelli, Solid State Electron. **30**, 345 (1987).
[47]G. Connell and W. Paul, J. Non-Cryst. Solids **8–10**, 215 (1972).
[48]W. Beyer, J. Non-Cryst. Solids **97–98**, 1027 (1987).
[49]W. Beyer, R. Hager, H. Schmidbaur, and G. Winterling, Appl. Phys. Lett. **54**, 1666 (1989).
[50]D. A. Papaconstantopoulos and E. N. Economou, Phys. Rev. B **24**, 7233 (1981).
[51]J. A. Vergés, Phys. Rev. Lett. **53**, 2270 (1984).
[52]D. C. Allan and J. D. Joannopoulos, Phys. Rev. Lett. **44**, 43 (1980).
[53]G. Allan, C. Delerue, and M. Lannoo, Phys. Rev. B **57**, 6933 (1998).
[54]M. Peressi, L. Colombo, and S. de Gironcoli, Phys. Rev. B **64**, 193303 (2001).
[55]M. Tosolini, L. Colombo, and M. Peressi, Phys. Rev. B **69**, 075301 (2004).
[56]F. Wooten, K. Winer, and D. Weaire, Phys. Rev. Lett. **54**, 1392 (1985).
[57]C. G. Van de Walle, Phys. Rev. B **39**, 1871 (1989).
[58]L. H. Yang, C. Y. Fong, and C. S. Nichols, Phys. Rev. Lett. **66**, 3273 (1991).
[59]M. Schmidt, L. Korte, A. Laades, R. Stangl, C. Schubert, H. Angermann, E. Conrad, and K. Maydell, Thin Solid Films **515**, 7475 (2007).
[60]G. D. Cody, T. Tiedje, B. Abeles, B. Brooks, and Y. Goldstein, Phys. Rev. Lett. **47**, 1480 (1981).
[61]A. H. M. Smets, W. M. M. Kessels, and M. C. M. van de Sanden, Appl. Phys. Lett. **82**, 865 (2003).
[62]M. H. Brodsky, M. Cardona, and J. J. Cuomo, Phys. Rev. B **16**, 3556 (1977).
[63]K. K. Gleason, M. A. Petrich, and J. A. Reimer, Phys. Rev. B **36**, 3259 (1987).
[64]C. Manfredotti, F. Fizzotti, M. Boero, P. Pastorino, P. Polesello, and E. Vittone, Phys. Rev. B **50**, 18046 (1994).
[65]Y. Wu, J. T. Stephen, D. X. Han, J. M. Rutland, R. S. Crandall, and A. H. Mahan, Phys. Rev. Lett. **77**, 2049 (1996).
[66]A. H. M. Smets and M. C. M. van de Sanden, Phys. Rev. B **76**, 073202 (2007).
[67]H. Wagner and W. Beyer, Solid State Commun. **48**, 585 (1983).
[68]C. M. Soukoulis, M. H. Cohen, and E. N. Economou, Phys. Rev. Lett. **53**, 616 (1984).
[69]P. A. Fedders, D. A. Drabold, and S. Nakhmanson, Phys. Rev. B **58**, 15624 (1998).
[70]J. Dong and D. A. Drabold, Phys. Rev. Lett. **80**, 1928 (1998).
[71]Y. Pan, F. Inam, M. Zhang, and D. A. Drabold, Phys. Rev. Lett. **100**, 206403 (2008).
[72]S. Chakraborty and D. A. Drabold, Phys. Rev. B **79**, 115214 (2009).